Published in final edited form as:
Metabolism. 2013 January ; 62(1): 152–162. doi:10.1016/j.metabol.2012.07.012.

Hepatic Glucose Production Pathways after Three Days of a High-fat Diet

Eunsook S. Jin[1,2,*], **Sara A. Beddow**[3], **Craig R. Malloy**[1,2,4,5], and **Varman T. Samuel**[3,6]

[1]Advanced Imaging Research Center, University of Texas Southwestern Medical Center, Dallas, TX 75390

[2]Department of Internal Medicine, University of Texas Southwestern Medical Center, Dallas, TX 75390

[3]Yale University School of Medicine, New Haven, CT 06515

[4]Department of Radiology, University of Texas Southwestern Medical Center, Dallas, TX 75390

[5]VA North Texas Health Care System, Dallas, TX 75216

[6]VA Connecticut Health Care System, West Haven, CT 06516.

Abstract

Objective—A three-day high-fat diet induces hepatic steatosis and hepatic insulin resistance in rats without altering fasting plasma glucose concentration or the rate of glucose production. However, as the nutrient profile available to the liver is substantially altered by a high-fat diet, we hypothesized that the relative fluxes supporting hepatic glucose production would be altered.

Materials/Methods—To test this hypothesis, we used multiple tracers ([3,4-$^{13}C_2$]glucose, ^2H_2O, and [U-$^{13}C_3$]propionate) followed by NMR analysis of blood glucose to quantify net glucose production and the contributions of glycogen and key gluconeogenesis precursors in 4-5-hour fasted rats.

Results—NMR analysis demonstrated that the majority of blood glucose was derived from glycogen and the citric acid cycle, while a smaller fraction of glucose was derived from glycerol in both controls and high-fat-fed animals. High-fat feeding was associated with a two-fold increase in plasma glycerol concentration and an increase in the contribution (both fractional and absolute) of glycerol-gluconeogenesis. The increase in gluconeogenesis from glycerol tended to be balanced by a decrease in glycogenolysis. The absolute fluxes associated with the citric acid cycle including gluconeogenesis from the cycle intermediates, pyruvate cycling and citric acid cycle flux itself, were not altered by this short high-fat diet.

*Corresponding author: University of Texas Southwestern Medical Center 5323 Harry Hines Blvd. Dallas, TX 75390-8568 Telephone: 214-645-2725, FAX: 214-645-2744 eunsook.jin@utsouthwestern.edu.

CONFLICT OF INTEREST None of the authors have competing financial interests to declare.

AUTHORSHIP ESJ and VTS designed and performed the research, analyzed the data, and wrote the paper. SAB performed the study and collected the data. CRM designed the research, analyzed the data, and wrote the paper.

Conclusions—A short term high-fat diet altered the specific pathways for hepatic glucose production without influencing the overall rate of glucose production or flux in the citric acid cycle.

Keywords

high-fat diet; glycerol; hepatic insulin resistance; NMR; glucose production

INTRODUCTION

Hepatic glucose production is supported by the sum of flux through glycogenolysis, gluconeogenesis from glycerol, and gluconeogenesis from intermediates of the citric acid cycle. Fluxes through these individual pathways are sensitive to multiple factors such as dietary fat content or diseases such as type 2 diabetes or nonalcoholic fatty liver disease. For example, fasting hyperglycemia among patients with type 2 diabetes has been attributed to hepatic glucose over-production, but the contribution from glycerol, glycogen or the citric acid cycle remains controversial. Several studies reported elevated glycogenolysis and increased liver glycogen contents in patients with diabetes and in obese subjects [1-3] while other studies using ^{13}C magnetic resonance spectroscopic analysis reported the opposite [4-6]. In animal models, Zucker diabetic fatty rats had dramatically higher hepatic glycogen after a 24-hr fast compared to controls and they had substantially increased glycogenolysis contributing to fasting hyperglycemia [7]. Mouse models of diabetes, ob/ob and db/db mice, were also reported to have increased hepatic glycogen [8-10].

The effect of diet on glucose production has also been examined. In rodents, a short term high-fat diet causes hepatic steatosis and hepatic insulin resistance, without the confounding effects of peripheral insulin resistance [11, 12]. Using this model, we have shown that hepatic insulin resistance is associated with accumulation of hepatic diacylglycerol and PKCε activation, which in turn impairs insulin signaling [13, 14]. Though this short term diet clearly induced hepatic insulin resistance, basal, fasting plasma glucose concentration and the rate of endogenous glucose production (EGP) were unchanged [13]. However, since glucose production is supported by multiple sources, the contribution of these fluxes may be altered following this dietary intervention. It is also worth emphasizing that flux through specific pathways may not correlate closely with expression of the putative controlling enzymes [15]. For example, up-regulation of phospho*enol*pyruvate carboxykinase (PEPCK) expression after a 12-week high-fat diet [16] may not mean the same degree of PEPCK flux or not even glucose production. Burgess et al reported that substantial reduction of hepatic PEPCK contents caused only small changes in the flux through PEPCK [17]. As another example, Zucker diabetic fatty rats have increased expression of PEPCK and increased glucose production [7, 18]. Yet when probing the metabolic network that supports glucose production, we observed that the increased flux from oxaloacetate (OAA) to phospho*enol*pyurvate (PEP) was balanced by an increase in flux from PEP back to pyruvate. Together these changes prevented a net contribution of PEP to glucose [7]. In general, the gene expression profile is a poor indicator of metabolic fluxes; these must be measured directly.

High-fat feeding will increase lipid turnover and may lead to increased rates of lipolysis and subsequently increased concentrations of non-esterified fatty acids (NEFAs) and glycerol [19-22]. Glycerol appearance was increased in rats fed on a high-fat diet for 8 weeks [22], and glycerol was suggested to be the most important precursor in adding new carbons for glucose pool in type 2 diabetes [23, 24]. Since the rate of gluconeogenesis from glycerol was reported to be proportional to plasma glycerol [23], increased gluconeogenesis would be expected after a brief high-fat diet. It is possible that a three-day high-fat diet may increase

the contribution in some fluxes that are balanced by decreases in others, thus preserving normal basal glucose production.

The goal of the present study was to assess the effect of a brief high-fat diet on all fluxes in the pathways involved in glucose production. Metabolic fluxes were estimated using three stable isotope tracers: [3,4-$^{13}C_2$]glucose for glucose turnover measurement [25], ^2H_2O for the measurement of fractional contributions of glycogenolysis, gluconeogenesis from glycerol, and gluconeogenesis from the citric acid cycle to EGP [26, 27], and [U-$^{13}C_3$]propionate for the measurement of fluxes related to the citric acid cycle [28]. Three-day High-fat feeding increased both plasma glycerol and hepatic triglycerides in rats without change in plasma glucose, hepatic glucose production, or citric acid cycle flux in the liver. However, flux through glycerol gluconeogenesis was increased significantly by this brief diet.

METHODS

Materials

[3,4-$^{13}C_2$]glucose (99%) was purchased from Omicron Biochemicals (South Bend, IN). [U-$^{13}C_3$]propionate (99%), ^2H_2O (99.9%) and deuterated acetonitrile (99.8%) were obtained from Cambridge Isotopes (Andover, MA). Other common chemicals were purchased from Sigma-Aldrich (St. Louis, MO).

Pathways Supporting Glucose Production

The study of glucose production pathways was approved by the Institutional Animal Care and Use Committee at the University of Texas Southwestern Medical Center. Male Sprague-Dawley rats were purchased from Charles River Laboratories. The rats were placed on a 12-h day/night cycle and provided ad-libitum access to food and water, except when specified by experimental protocol. One week before the study day, catheters were inserted into the right internal jugular vein, extending to the right atrium under general anesthesia and the animals were allowed to recover for seven days. Upon recovery from the surgery, one group of rats (n=9) was switched to a high-fat diet with 60% calories provided from fat, 20% from carbohydrate and 20% from protein (5.24 kcal/g; cat. no. D12492; Research Diets inc., New Brunswick, NJ) for three days before the study day. Lard and soybean were the fat sources (lard:soybean = 9:1 in kcal) for the high-fat diet. The other group (n=9) continued a standard chow diet with 12% calories provided from fat, 66% from carbohydrate and 22% from protein (3.0 kcal/g; cat. no. 2016; Teklad FG rodent diet, Harlan Teklad). Soybean was the main fat source for the standard diet. The three-day high-fat diet did not induce body weight difference between two groups (324 ± 4 g in controls vs. 338 ± 8 g in high-fat diet; 12-week-old rats). On the study day, rats were fasted for 4-5 hrs beginning at 8:00 a.m. with free access to water. At t = -20 min, rats received an intravenous bolus injection of ^2H_2O-[U-$^{13}C_3$]propionate mixture (7.5 μL/g rat, 13 mg [U-$^{13}C_3$]propionate/mL ^2H_2O) over 10 minutes through the indwelling catheter. At t =0, rats received a bolus infusion of [3,4-$^{13}C_2$]glucose (35 μmol/kg) followed by continuous infusion of the tracer (1μmol/kg/min) *via* the catheter for 90 min. At the end of the infusion, whole blood (~8-10 mL) was drawn from the inferior vena cava under anesthesia with sodium pentobarbital (50 mg/kg body wt). A small portion of whole blood (~1mL) was used for metabolite assays and the remaining major portion was used for glucose isolation for NMR analysis. Liver and skeletal muscle tissues from the hind limbs were freeze-clamped and kept under −80°C for subsequent processing.

Sample processing for NMR analysis

Blood was immediately centrifuged, and plasma supernatant was deproteinized by adding cold perchloric acid to a final concentration of 7% by volume. After neutralization with KOH and centrifugation, the supernatant was lyophilized. To convert plasma glucose into monoacetone glucose (MAG; Figure 1), the dried residue was suspended in 3.0 ml of acetone containing 120 μl of concentrated sulfuric acid. The mixture was stirred for 4 h at room temperature to yield diacetone glucose. After filtering off particulates and adding 3 ml of water, we adjusted the pH to 2.0 by dropwise addition of 1.5 M Na_2CO_3. The mixture was stirred for 24 h at room temperature to convert diacetone glucose into MAG. The pH was then further increased to ~8.0 by dropwise addition of Na_2CO_3. Acetone was evaporated under a vacuum, and the sample was freeze-dried. MAG was extracted into 3 ml (5x) of hot ethyl acetate, the solutions were combined, and the ethyl acetate was removed by vacuum evaporation. The resulting MAG was further purified by passage through a 3-ml DSC-18 cartridge, using 5% acetonitrile as eluant. The effluent was freeze-dried and stored dry before NMR analysis.

Glycogen from liver tissues (~8 g) or skeletal muscle tissues (~ 8 g) was extracted and purified as described previously [29]. The hydrolysis of purified glycogen was performed by dissolving in 5 ml of 10 mM sodium acetate solution (pH 4.8) and incubating with amyloglucosidase (50 mg glycogen/20 U amyloglucosidase) for 4 h at 50°C. After freeze-drying, the hydrolyzed glycogen was converted to MAG as described above.

NMR Spectroscopy

All NMR spectra were collected using a Varian Inova 14.1-T spectrometer (Varian Instruments, Palo Alto, CA, USA) equipped with a 3-mm broadband probe with the observe coil tuned to ^{1}H (600 MHz), ^{2}H (92 MHz), or ^{13}C (150 MHz). After shimming performed on selected ^{1}H resonances of MAG, proton-decoupled ^{2}H NMR spectra were acquired using a 90° pulse (12.5 μs), 920 Hz sweep width, 1836 of data points, and a 1-s acquisition time with no further delay at 50°C. Spectra were averaged 10,000 - 70,000 scans requiring ~3-18 h. Proton decoupling was performed using a standard WALTZ-16 pulse sequence. ^{13}C NMR spectra of MAG samples were collected using 52° pulse (6.06 μs), 20,330 Hz sweep, with 60,992 data points, and a 1.5-s acquisition time with no further delay at 25°C. Typically 4,000 - 40,000 scans were averaged, requiring ~2-18 h. NMR spectra were analyzed using ACD/Labs PC-based NMR spectral analysis program (Advanced Chemistry Development, Inc., Toronto, Canada).

Glucose turnover and Metabolic Fluxes

Glucose turnover was estimated from the dilution of infused [3,4-$^{13}C_2$]glucose, using ^{13}C NMR to analyze MAG derived from plasma glucose at the end of the infusion protocol (Figure 1). Briefly, the fraction of [3,4-$^{13}C_2$]glucose in plasma glucose was determined from the ratio of the areas of the doublet due to J_{34} (^{13}C-^{13}C spin-spin couplings in carbons 3 and 4) in carbon 3 at 75.3 parts/million (ppm) and in carbon 4 at 80.5 ppm compared with the total area of the two methyl resonances at 26.1 and 26.7 ppm. Because the methyl resonances reflect natural abundance ^{13}C, the fraction of [3,4-$^{13}C_2$]glucose in MAG was evaluated based on standard curves [25]. Glucose production was calculated from the known infusion rate (R_i), the fraction of infusate glucose that was [3,4-$^{13}C_2$]glucose (L_i), and the fraction of plasma glucose that was [3,4-C_2]glucose (L_p) at the end of the infusion period

$$\text{v1=glucose production}=R_i \bullet \left(L_i - L_p\right)/L_p$$

Flux from glycogen, glycerol, and PEP (or the citric acid cycle) into plasma glucose was estimated from the deuterium (^2H) enrichment at positions 2, 5, and 6_s (H2, H5, and $H6_s$, respectively), as determined from the ^2H NMR of MAG (Figure 2)

$$v2=\text{flux from glycogen}=v1 \bullet (H2 - H5)/H2$$

$$v3=\text{flux from glycerol}=2 \bullet v1 \bullet (H5 - H6_s)/H2$$

$$v4=\text{flux from PEP (or the citric acid cycle)}=2 \bullet v1 \bullet H6_s/H2$$

A ^{13}C NMR isotopomer analysis based on the ^{13}C-^{13}C spin-spin coupled multiplets of carbon 5 of MAG (Figure 3) has been reported previously [28] that yields relative fluxes in the citric acid cycle as follows

$$v4/v7=(C5Q - C5D45)/C545$$

$$v5/v7=(C5D56 - C5Q)/C5D45$$

$$v6/v7=(C5D56 - C5D45)/C5D45$$

where the variables C5Q, C5D56, and C5D45 are the areas of the quartet, doublet due to J_{56}, and doublet due to J_{45}, relative to the area of the carbon 5 resonance. The assumptions in the metabolic model include the following: *1*) all glucose originates from the liver, *2*) hydrolytic conversion of glycogen to glucose via amylo-1,6-glucosidase is negligible, *3*) there is insignificant labeling of acetyl-CoA entering the TCA cycle from either tracer [3,4-$^{13}C_2$]glucose or [U-$^{13}C_3$]propionate, *4*) there is complete equilibration of all ^{13}C-enriched four-carbon intermediates in the citric acid cycle, and *5*) steady-state metabolic conditions apply [28].

[3,4-$^{13}C_2$]glucose is an ideal tracer of glucose turnover for use in combination with [U-$^{13}C_3$]propionate as a tracer of the citric acid cycle. The metabolism of [3,4-$^{13}C_2$]glucose to the level of a triose followed by resynthesis to glucose yields only [3-^{13}C]glucose or [4-^{13}C]glucose, since the absolute enrichment of the triose pool is low and *de novo* generation of [3,4-$^{13}C_2$]glucose is negligible. Another important aspect of this glucose tracer is that any metabolism of [3,4-$^{13}C_2$]glucose to pyruvate followed by carboxylation to OAA, continued metabolism in the citric acid cycle, and resynthesis to glucose can only produce [3-$^{13}C_1$]glucose or [4-$^{13}C_1$]glucose. This feature means that ^{13}C enrichment patterns in glucose carbons 1 and 2 or 5 and 6 can only be derived from metabolism of [U-$^{13}C_3$]propionate.

Each variable used to describe the metabolic results (v1–v7) generally describes the combined actions of multiple enzyme-catalyzed reactions. For example, v2 indicates the rate of generation of glucose 6-phosphate from glycogen, without implying measurement of flux in a specific reaction. Similarly, v5 is used to describe the flux of carbon skeletons from the PEP/pyruvate pool through carboxylation and regeneration of OAA. Flux from OAA to

pyruvate to OAA can occur via the combined effects of either malate dehydrogenase, the malic enzyme and pyruvate carboxylase, or PEPCK, pyruvate kinase and pyruvate carboxylase. Hence, v5 simply designates the sum of fluxes through both pathways. Pyruvate carboxylase is common to both pathways, so v5 is also a lower limit on total flux through pyruvate carboxylase.

Metabolite Assays

Plasma glucose was assayed enzymatically [30]. Plasma NEFAs were measured using a commercially available kit (Wako Chemicals, Neuss, Germany). The levels of plasma glycerol, plasma triglycerides and liver triglycerides were determined using a kit from Sigma. Plasma insulin concentration was determined by a RIA Assay system (Linco). Liver tissues were pulverized under liquid nitrogen, and a portion (< 1 g) was extracted with perchloric acid (6%) and subsequently used for the enzymatic assays of glycogen, pyruvate and lactate [30].

Expression of Liver Enzymes

Total RNA was extracted from liver samples stored in RNAlater using the RNeasy kit (Qiagen). The abundance of transcripts for glucose 6-phosphatase, pyruvate carboxylase and PEPCK1 (cytosolic) was assessed by real time PCR using a SYBR Green detection system (Qiagen). For each run, samples were run in duplicates for both the gene of interest and actin. The expression data for each gene of interest and actin was normalized for the efficiency of amplification, as determined by a standard curve included on each run [31].

Statistical Analysis

The data are expressed as mean ± standard error (SE). Comparisons between high-fat-fed rats and controls were performed using one-way analysis of variance. Differences in mean values were considered statistically significant at a probability level of less than 5% ($p < 0.05$).

RESULTS

Effects of a High-Fat Diet on Metabolic Parameters

Three days of high-fat feeding increased liver triglyceride content ~ 7-fold and also increased plasma glycerol and insulin concentrations (Table 1). This dietary intervention induced hepatic insulin resistance, determined using a hyperinsulinemic-euglycemic clamp (data not shown), as reported previously [13]. However, the diet did not change body weight, plasma glucose, plasma triglyceride or NEFA concentration. Liver glycogen content in fat-fed animals tended to be decreased, but it did not reach statistical significance (p=0.14). There were no changes in lactate and pyruvate concentrations in liver between two groups.

Glucose Production, Storage and Disposal by ^{2}H and ^{13}C NMR Analysis

Under basal, fasted conditions, [3,4-$^{13}C_2$]glucose enrichment in the plasma was identical between two groups,1.27 ± 0.08% in control animals and 1.22 ± 0.10% in high-fat-fed animals (Table 1). Therefore, EGP was not different (Table 2). [3,4-$^{13}C_2$]glucose enrichment in muscle glycogen was the same in both groups (~0.05 - 0.06%; Table 1), but there was no excess ^{13}C enrichment in liver glycogen above natural abundance in either group. Similarly ^{2}H labeling at the H2 position of glucosyl units of liver glycogen was at natural abundance. Together these findings demonstrate that no glucose generated from either glycerol or the citric acid cycle was stored in liver glycogen. Consequently, all glucose produced by the liver was exported into the blood under these conditions.

Sources of Plasma Glucose by ^{2}H NMR Analysis

The relative ^{2}H enrichments in H2, H5 and $H6_s$ of blood glucose provide the fractional contributions of glycogen, glycerol, and the citric acid cycle (or PEP) to glucose production [26]. Typical ^{2}H NMR spectra of MAG, derived from plasma glucose, are shown in Figure 2 for both control and high-fat-fed animals (Figures 2A & 2B). The difference in ^{2}H enrichments in position 2 and position 5 demonstrates that a substantial fraction of blood glucose was derived from glycogenolysis. The presence of large signal in the H6 position also indicates that a significant fraction of glucose was derived from carbons originating in the citric acid cycle. In comparison, the difference in ^{2}H enrichments in position 5 and position 6 indicates that the overall contribution of glycerol to glucose production was small. Nevertheless, the fractional glycerol contribution was slightly higher in high-fat-fed rats ($p=0.05$, 0.15 ± 0.01 in controls vs. 0.19 ± 0.01 in high-fat-fed rats) while fractional glycogen contribution tended to be slightly lower in those rats ($p=0.08$, 0.48 ± 0.02 in controls vs. 0.41 ± 0.02 in high-fat-fed rats). Fractional contribution from the citric acid cycle was not different between two groups (Figure 2C). The absolute rates of glucose production from glycogen, PEP, and glycerol were determined by multiplying the individual fractional contributions and the glucose production rates (Table 2 and Figure 4). High-fat feeding increased the contribution of glycerol-gluconeogenesis ($p = 0.029$, 23.7 ± 1.6 μmol/kg/min vs. 31.2 ± 2.7 μmol/kg/min). In contrast, gluconeogenesis from the citric acid cycle was similar between two groups and the tendency of decreased glycogenolysis in high-fat-fed rats did not reach statistical significance.

Citric Acid Cycle and Related Fluxes by ^{13}C NMR Analysis of Blood Glucose

Entry of [U-$^{13}C_3$]propionate into the citric acid cycle (Figure 4) and subsequent turnover produces a mixture of ^{13}C isotopomers in all intermediates of the cycle, and the relative concentrations of these isotopomers are sensitive to pyruvate cycling, anaplerosis and gluconeogenesis. The ^{13}C labeling pattern in carbons 4, 5 and 6 of glucose correspond to the labeling pattern in carbons 1, 2 and 3 of oxaloacetate, respectively [28]. Analysis of glucose C5 multiplets (Figures 3A & 3B) provides an estimate of fluxes through PEPCK, pyruvate cycling and gluconeogenesis through PEP, all relative to citrate synthase (CS) flux. PEPCK/CS tended to be higher in high-fat-fed rats ($p=0.05$, 1.53 ± 0.15 vs. 1.88 ± 0.09) and similar trends were found in gluconeogenesis/CS and pyruvate cycling/CS, but they did not reach statistical significance (Table 2 & Figure 3C). Fluxes through the individual glucose production pathways can be calculated by combining the rate of glucose production, fractional sources of glucose production by ^{2}H NMR analysis and the fluxes involving the citric acid cycle by ^{13}C NMR analysis, each measured individually in a single animal. No differences were observed in absolute fluxes related to the citric acid cycle such as PEPCK pathway, pyruvate cycling and the citric acid cycle itself between two groups (Table 2 and Figure 4).

Expressions of Liver Enzymes

We assessed the expression of key gluconeogenic enzymes in the liver. There was no statistically difference in the mRNA levels of liver enzymes including glucose 6-phosphatase, pyruvate carboxylase and PEPCK1 (cytosolic) between two groups (Figure 5).

DISCUSSION

The current study confirmed our earlier observation that development of hepatic steatosis and hepatic insulin resistance following a three-day high-fat diet does not lead to either hyperglycemia or increased rates of glucose production [13]. However, we hypothesized that the change in dietary substrates would alter the balance of various pathways that support glucose production. To test this hypothesis, we quantified fluxes through all glucose-

producing pathways using a combination of stable isotope tracers. Specifically, $^{2}H_{2}O$ was used to assess the relative contributions of gluconeogenesis from the citric acid cycle, gluconeogenesis from glycerol and glycogenolysis, [U-$^{13}C_{3}$]propionate was used to assess fluxes associated with the citric acid cycle and [3,4-$^{13}C_{2}$]glucose was used to quantify glucose turnover. Carbon atoms in glucose became labeled from [3,4-$^{13}C_{2}$]glucose, and ^{13}Cs from [U-^{13} C_{3}]propionate, while protons became labeled by ^{2}Hs from $^{2}H_{2}O$. The distinctive labeling pattern of glucose from each tracer was easily identified by ^{2}H and ^{13}C NMR analysis of MAG. A short fasting duration (4-5-hr) was chosen in current study to better assess the pathways of hepatic glucose production when adequate glycogen was available to support glucose production, the normal physiological situation.

Since glycogen synthesis and degradation may occur simultaneously even in the fasted rat [32], we confirmed that under these conditions no glucose produced from either glycerol or the citric acid cycle was stored as glycogen. Consequently, the fluxes measured based on isotope distribution in plasma glucose reflect all gluconeogenic fluxes in the liver. While this short dietary intervention did not increase net basal hepatic glucose production, the fluxes supporting glucose production were altered with increased gluconeogenesis from glycerol. This finding is consistent with the observed increase in plasma glycerol concentration of high-fat-fed rats. This suggests that a failure to suppress lipolysis leads to higher circulating glycerol concentration which is transported into hepatocytes where it can be converted into triose phosphates (dihydroxyacetone phosphate and glyceraldehyde 3-phosphate) and participating in gluconeogenesis [33].

The current study demonstrated that increased glycerol-gluconeogenesis was a very early metabolic change associated with a high-fat diet. A three-day high-fat diet induced hyperinsulinemia, which may prevent basal hepatic glucose over-production and subsequently maintained glucose homeostasis. However, it did not suppress glycerol-gluconeogenesis among the supporting fluxes of glucose production presumably due to the increased lipolysis after a high-fat diet, which supplied glycerol to the liver as a gluconeogenic substrate. The increased plasma glycerol concentration in high-fat-fed rats supports this view. This alteration was presumably due to diet composition switch rather than excess calorie intake because rats on a high-fat diet had similar total calorie intake with controls based on our previous observation and reports by others [13, 22].

The carbons of glucose can originate from discrete sources that are very different. For example, glycogen is a condensed form of glucose while lactate and pyruvate, the sources of carbon skeletons for the citric acid cycle, largely represent carbons produced from extrahepatic glycolysis. In contrast, glycerol carbons are essentially from lipids. From this perspective, glycerol is a unique source for adding new carbons to the glucose pool [23]. Glycerol could be oxidized through the citric acid cycle or utilized in gluconeogenesis if not consumed in lipogenesis. The current study showed that a brief high-fat diet directed glycerol into gluconeogenic process. We speculate that high-fat feeding increased fatty acid oxidation after the diet [19] and consequently spared glycerol and carbohydrates from being oxidized.

The net hepatic glucose production was not altered in this study despite the clear-cut increased contribution of glycerol to gluconeogenesis. It should be emphasized that the quantitative contribution of glycerol to glucose production was modest in both groups, less than 20% of glucose production, so it may be difficult to detect a reciprocal change in other pathways. We did observe a trend of decreased glycogenolysis in the high-fat-fed animas, consistent with that of decreased liver glycogen contents in these animals (Table 1) which was presumably related to the low carbohydrate intake of the diet.

The entry of glycerol into gluconeogenesis bypasses several key checkpoints in the pathway, such as pyruvate carboxylase and PEPCK. A three-day high-fat diet did not induce noticeable changes of PEPCK and other absolute fluxes related to the citric acid cycle. These observations were consistent with the lack of changes in mRNA expression of liver enzymes including pyruvate carboxylase and PEPCK1 (cytosolic). However, PEPCK flux relative to citrate synthase flux (PEPCK/CS) tended to increase at the border line of statistical significance ($p=0.05$), and pyruvate cycling/CS and gluconeogenesis/CS also showed a similar trend (Figure 3C). A three-day high-fat diet did not have substantial impact on fluxes associated with the citric acid cycle, but this study suggests that subtle changes occurred in those fluxes by the short dietary intervention.

The low carbohydrate intake in high-fat-fed animals was associated with a trend to lower glycogenolysis, as noted. This trend is minor in the aspect that the animal received substantially low calorie from carbohydrates. Increased fatty acid oxidation after a high-fat diet [19] could spare carbohydrates from being oxidized. There was no difference in glycogen synthesis in two groups based on ^{13}C and ^{2}H distributions in tissue glycogen. Because [3,4-$^{13}C_2$]glucose enrichment in blood glucose is the same in both groups, glycogen synthesis *via* the direct pathway (glucose -> glucose 6-phosphate -> UDP-glucose -> glycogen) can be measured by assessing [3,4-$^{13}C_2$]glucose enrichment in tissue glycogen. The excess enrichment of [3,4-$^{13}C_2$]glucose in skeletal muscle glycogen (~0.05 - 0.06%) demonstrated that blood glucose was phosphorylated and converted to glycogen, but the degree of this conversion was the same in both groups.

In contrast to current study, longer durations of high-fat feeding have been reported to increase body weight, increase plasma glucose, increase hepatic glucose production and citric acid cycle flux [22, 34, 35]. However, the length of diet needed for those changes were quite varied among studies; for instance, 2-week was reported to induce glucose over-production by a study in rodents [34] while another reported that even 8-week intervention was not enough to cause such a change [35]. Glucose over-production after longer durations was attributed to increased gluconeogenesis, but interestingly increased hepatic glycogen levels were also observed in rats after a 2-week high-fat diet [34, 35]. Longer high-fat diets also increased PEPCK expression [16, 36] and induced the citric acid cycle intermediates such as fumarate and citrate in liver of mice [37]. These changes were not observed in current study, but there are some similarity between current study and studies with longer high-fat diets. Podolin et al. reported elevated glycerol-gluconeogenesis after 8-week high-fat feeding [22], and longer durations also increased glycerol appearance and lipolysis [22, 34, 35]. The current study is unique because it identified early disruptions induced by a high-fat diet prior to substantial overall changes by longer high-fat feeding.

[U-$^{13}C_3$]propionate has been used to report relative fluxes associated with the citric acid cycle. After the tracer incorporation into the cycle, subsequent processes through metabolic pathways including pyruvate cycling and anaplerosis reflected in the labeling patterns in oxaloacetate C1-C3, which were reserved in glucose C1-C3 and glucose C4-C6 [28]. We chose glucose C4-C6 rather than C1-C3 in this study to estimate the relative fluxes. The labeling patterns between glucose C1-C3 and C4-C6 (i.e., MAG C2 and C5 resonances, respectively) were slightly different in rats after a 4-5-h fast, presumably due to the activity of pentose phosphate pathway (PPP). In the absence of PPP, the relative peak areas of corresponding peaks should be the same (D12=D56, C2Q=C5Q and D23=D45) because glucose C1-C3 and C4-C6 have the common intermediate, oxaloacetate C1-C3. However, NMR analysis showed ^{13}C asymmetry in glucose characterized by C2D12 > C5D56 and C2Q < C5Q (Figure 6A). It could be explained by rearrangement of glucose C1-C3 through PPP activity. For example, when [1,2,3-$^{13}C_3$]glucose 6-phosphate is involved in the PPP, the ^{13}C of C1 position is lost through the oxidative phase, becoming [1,2-$^{13}C_2$]fructose 6-

phosphate (Figure 6B). This process decreases [1,2,3-$^{13}C_3$]glucose while increases [1,2-$^{13}C_2$]glucose, simultaneously. In contrast, labeling patterns at glucose C4-C6 remain the same even in the presence of PPP activity, reflecting the patterns in oxaloacetate C1-C3.

In summary, while a three-day high-fat diet does not alter net basal hepatic glucose production, it does alter the contribution of the supporting fluxes. Specifically, we observed an increase in glycerol-gluconeogenesis that may be a consequence of increased peripheral lipolysis and increased glycerol delivery to the liver. Future studies will determine whether similar changes are present under hyperinsulinemic-euglycemic conditions and assess the relative roles of hepatic insulin resistance versus adipocyte insulin resistance in altering these flux pathways. These *in vivo* metabolic studies of quantifying the fluxes that contribute to gluconeogenesis will improve our understanding about the development of hepatic insulin resistance and be useful to find a better treatment to relieve hepatic glucose over-production.

Acknowledgments

We thank Charles Storey and Angela Milde for performing the animal studies. We thank Yanna Kosover and the Yale DERC Hormone Assay labs for their technical assistance.

FUNDING ESJ was supported by a N.I.H. grant (DK078933). CRM was supported by a N.I.H. grant (RR-02584). VTS was supported by a VA Merit Review Award.

ABBREVIATIONS

CS	citrate synthase
DHAP	dihydroxyacetone phosphate
EGP	endogenous glucose production
FBP	fructose 1,6-bisphosphate
FUM	fumarate
F6P	fructose 6-phosphate
GA3P	glyceraldehyde 3-phosphate
GNG	gluconeogenesis
G6P	glucose 6-phosphate
G6Pase	Glucose 6-phosphatase
HFD	high-fat diet
MAG	monoacetone glucose
MAL	malate
ME	malic enzyme
NEFAs	non-esterified fatty acids
NMR	nuclear magnetic resonance
OAA	oxaloacetate
PCR	polymerase chain reaction
PEP	phospho*enol*pyruvate
PEPCK	phospho*enol*pyruvate carboxykinase

PK	pyruvate kinase
PKC	protein kinase C
ppm	parts/million
PPP	pentose phosphate pathway
SUCC	succinyl-CoA

REFERENCES

[1]. Basu R, Schwenk WF, Rizza RA. Both fasting glucose production and disappearance are abnormal in people with “mild” and “severe” type 2 diabetes. Am J Physiol Endocrinol Metab. 2004; 287:E55–E62. [PubMed: 14982753]

[2]. Clore JN, Post EP, Bailey DJ, et al. Evidence for increased liver glycogen in patients with noninsulin-dependent diabetes mellitus after a 3-day fast. J Clin Endocrinol Metab. 1992; 74:660–6. [PubMed: 1740502]

[3]. Muller C, Assimacopoulos-Jeannet F, Mosimann F, et al. Endogenous glucose production, gluconeogenesis and liver glycogen concentration in obese non-diabetic patients. Diabetologia. 1997; 40:463–8. [PubMed: 9112024]

[4]. Magnusson I, Rothman DL, Katz LD, et al. Increased rate of gluconeogenesis in type II diabetes mellitus: a ^{13}C nuclear magnetic resonance study. J Clin Invest. 1992; 90:1323–7. [PubMed: 1401068]

[5]. Hundal RS, Krssak M, Dufour S, et al. Mechanism by which metformin reduces glucose production in type 2 diabetes. Diabetes. 2000; 49:2063–9. [PubMed: 11118008]

[6]. Kunert O, Stingl H, Rosian E, et al. Measurement of fractional whole-body gluconeogenesis in humans from blood samples using ^{2}H nuclear magnetic resonance spectroscopy. Diabetes. 2003; 52:2475–82. [PubMed: 14514629]

[7]. Jin ES, Park BH, Sherry AD, et al. Role of excess glycogenolysis in fasting hyperglycemia among pre-diabetic and diabetic Zucker (fa/fa) rats. Diabetes. 2007; 56:777–785. [PubMed: 17327448]

[8]. Harris RB, Zhou J, Redmann SM Jr, et al. A leptin dose-response study in obese (ob/ob) and lean (+/?) mice. Endocrinology. 1998; 139(1):8–19. [PubMed: 9421392]

[9]. Berglund ED, Li CY, Bina HA, et al. Fibroblast growth factor 21 controls glycemia via regulation of hepatic glucose flux and insulin sensitivity. Endocrinology. 2009; 150(9):4084–93. [PubMed: 19470704]

[10]. Zhang Y, Lee FY, Barrera G, et al. Activation of the nuclear receptor FXR improves hyperglycemia and hyperlipidemia in diabetic mice. Proc Natl Acad Sci U S A. 2006; 103(4): 1006–11. [PubMed: 16410358]

[11]. Cruciani-Guglielmacci C, Vincent-Lamon M, Rouch C, et al. Early changes in insulin secretion and action induced by high-fat diet are related to a decreased sympathetic tone. Am J Physiol Endocrinol Metab. 2005; 288:E148–E154. [PubMed: 15353406]

[12]. Kraegen EW, Clark PW, Jenkins AB, et al. Development of muscle insulin resistance after liver insulin resistance in high-fat-fed rats. Diabetes. 1991; 40:1397–1403. [PubMed: 1936601]

[13]. Samuel VT, Liu ZX, Qu X, et al. Mechanism of hepatic insulin resistance in non-alcoholic fatty liver disease. J Biol Chem. 2004; 279:32345–32353. [PubMed: 15166226]

[14]. Savage DB, Choi CS, Samuel VT, et al. Reversal of diet-induced hepatic steatosis and hepatic insulin resistance by antisense oligonucleotide inhibitors of acetyl-CoA carboxylases 1 and 2. J Clin Invest. 2006; 116:817–824. [PubMed: 16485039]

[15]. Magnuson MA, She P, Shiota M. Gene-altered Mice and Metabolic Flux Control. J Biol Chem. 2003; 278:32485–32488. [PubMed: 12788933]

[16]. Wu M, Wang X, Duan Q, Lu T. Arachidonic acid can significantly prevent early insulin resistance induced by a high-fat diet. Ann Nutr Metab. 2007; 51:270–276. [PubMed: 17622786]

[17]. Burgess SC, He T, Yan Z, et al. Cytosolic phosphoenolpyruvate carboxykinase does not solely control the rate of hepatic gluconeogenesis in the intact mouse liver. Cell Metab. 2007; 5:313–320. [PubMed: 17403375]

[18]. Muñoz MC, Barberà A, Domínguez J, et al. Effects of tungstate, a new potential oral antidiabetic agent, in Zucker diabetic fatty rats. Diabetes. 2001; 50:131–138. [PubMed: 11147778]

[19]. Ciapaite J, van den Broek NM, Te Brinke H, et al. Differential effects of short- and long-term high-fat diet feeding on hepatic fatty acid metabolism in rats. Biochim Biophys Acta. 2011; 1811:441–451. [PubMed: 21621638]

[20]. Gaidhu MP, Anthony NM, Patel P, et al. Dysregulation of lipolysis and lipid metabolism in visceral and subcutaneous adipocytes by high-fat diet: role of ATGL, HSL, and AMPK. Am J Physiol Cell Physiol. 2010; 298:C961–C971. [PubMed: 20107043]

[21]. Howe HR 3rd, Heidal K, Choi MD, et al. Increased adipose tissue lipolysis after a 2-week high-fat diet in sedentary overweight/obese men. Metabolism. 2011; 60:976–981. [PubMed: 21040937]

[22]. Podolin DA, Wei Y, Pagliassotti MJ. Effects of a high-fat diet and voluntary wheel running on gluconeogenesis and lipolysis in rats. J Appl Physiol. 1999; 86:1374–1380. [PubMed: 10194225]

[23]. Nurjhan N, Consoli A, Gerich J. Increased lipolysis and its consequences on gluconeogenesis in non-insulin-dependent diabetes mellitus. J Clin Invest. 1992; 89:169–175. [PubMed: 1729269]

[24]. Puhakainen I, Koivisto VA, Yki-Jarvinen H. Lipolysis and gluconeogenesis from glycerol are increased in patients with noninsulin-dependent diabetes mellitus. J Clin Endocrinol Metab. 1992; 75:789–794. [PubMed: 1517368]

[25]. Jin ES, Jones JG, Merritt M, et al. Glucose production, gluconeogenesis, and hepatic tricarboxylic acid cycle fluxes measured by nuclear magnetic resonance analysis of a single glucose derivative. Anal Biochem. 2004; 327:149–155. [PubMed: 15051530]

[26]. Jones JG, Solomon MA, Cole SM, et al. An integrated ^{2}H and ^{13}C NMR study of gluconeogenesis and TCA cycle flux in humans. Am J Physiol Endocrinol Metab. 2001; 281:E848–E856. [PubMed: 11551863]

[27]. Landau BR, Wahren J, Chandramouli V, et al. Contributions of gluconeogenesis to glucose production in the fasted state. J Clin Invest. 1996; 98:378–385. [PubMed: 8755648]

[28]. Jones JG, Naidoo R, Sherry AD, et al. Measurement of gluconeogenesis and pyruvate cycling in the rat liver: a simple analysis of glucose and glutamate isotopomers during metabolism of [1,2,3-$^{13}C_3$] propionate. FEBS Lett. 1997; 412:131–137. [PubMed: 9257705]

[29]. Moriwaki T, Landau BR. Sources of the carbon atoms of liver glycogen formed by cortisol administration to rats in vivo. Endocrinology. 1963; 72:134–145.

[30]. Bergmeyer, HU. Methods of Enzymatic Analysis. Academic Press; New York: 1974.

[31]. Pfaffl MW. A new mathematical model for relative quantification in real-time RT-PCR. Nucleic Acids Res. 2001; 29:e45. [PubMed: 11328886]

[32]. David M, Petit WA, Laughlin MR, et al. Simultaneous synthesis and degradation of rat liver glycogen. An in vivo nuclear magnetic resonance spectroscopic study. J Clin Invest. 1990; 86(2): 612–617. [PubMed: 2117024]

[33]. Patsouris D, Mandard S, Voshol PJ, et al. PPARalpha governs glycerol metabolism. J Clin Invest. 2004; 114:94–103. [PubMed: 15232616]

[34]. Song S, Andrikopoulos S, Filippis C, et al. Mechanism of fat-induced hepatic gluconeogenesis: effect of metformin. Am J Physiol Endocrinol Metab. 2001; 281(2):E275–E282. [PubMed: 11440903]

[35]. Satapati S, Sunny NE, Kucejova B, et al. Elevated TCA cycle function in the pathology of diet-induced hepatic insulin resistance and fatty liver. J Lipid Res. 2012; 53(6):1080–1092. [PubMed: 22493093]

[36]. Krajcovicová-Kudlácková M, Dibák O. Influence of the time of intake of a high fat diet on gluconeogenesis. Physiol Bohemoslov. 1985; 34:339–350. [PubMed: 2932754]

[37]. Kleemann R, van Erk M, Verschuren L, et al. Time-resolved and tissue-specific systems analysis of the pathogenesis of insulin resistance. PLoS One. 2010; 5:e8817. [PubMed: 20098690]

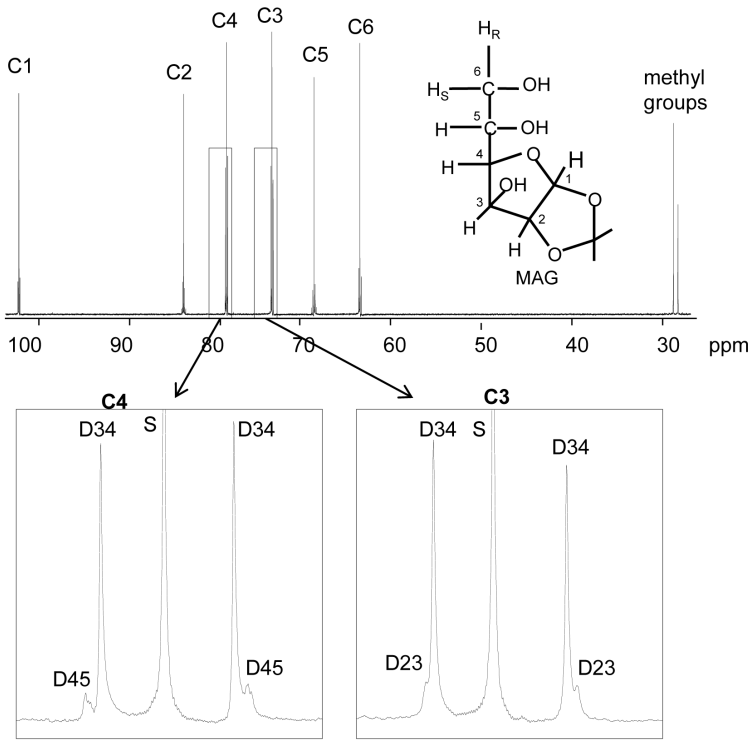

Figure 1.

^{13}C NMR spectrum of monoacetone glucose (MAG) derived from plasma glucose of a high-fat-fed animal and the chemical structure of MAG. The carbon sites in glucose are labeled from 1-6 (C1, C2, etc) in the spectrum. Two methyl groups of MAG were added during the conversion process from glucose to MAG, which are natural abundance. The spectrum around carbons 3 and 4 is expanded and shows doublets of carbon 3 and carbon 4 due to J_{34} in [3,4-$^{13}C_2$]glucose. Abbreviations: D34, doublet due to J_{34}; D45, doublet due to J_{45}; D23, doublet due to J_{23}; S, singlet.

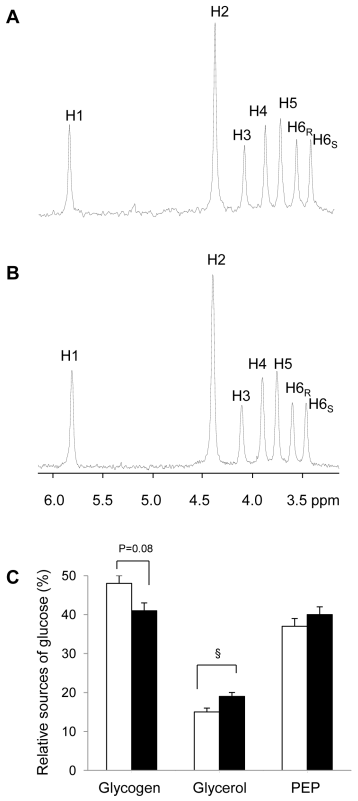

Figure 2.

^{2}H NMR spectra of MAG derived from plasma glucose of rats after a standard diet (**A**) and a high-fat diet (**B**). The hydrogen sites in glucose are labeled from 1 - 6 (H1, H2, etc.) in the spectra. ^{2}H NMR analysis informs the fractional contributions of glycogen, glycerol and the citric acid cycle (or PEP) to glucose production in controls (n=9, open bar) and high-fat-fed rats (n=9, black-filled bar; **C**). The difference between ^{2}H enrichments in position 2 and position 5 demonstrates that a substantial fraction of blood glucose was derived from glycogenolysis. The signal in the H6 position indicates the fraction of glucose derived from the citric acid cycle intermediates. The difference in ^{2}H enrichments in position 5 and position 6 indicates the contribution of glycerol to glucose production. (§, p =0.05).

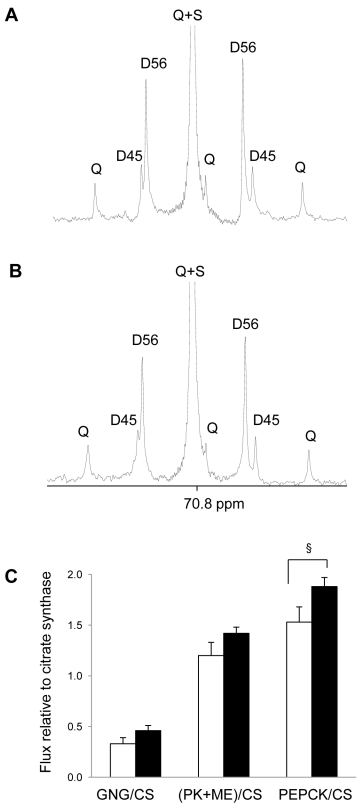

Figure 3.

^{13}C NMR spectra (carbon 5 region) of MAG derived from plasma glucose of rats after a standard diet (**A**) and a high-fat diet (**B**). The multiplets due to ^{13}C-^{13}C spin-spin couplings are labeled, which were analyzed to estimate fluxes associated with the citric acid cycle relative to citrate synthase flux (**C**) in controls (n=7, open bar) and high-fat-fed rats (n=9, black-filled bar). PK+ME represents pyruvate cycling. See the text for the details. Abbreviations: Q, quartet or doublet of doublets; D45, doublet due to J_{45}; D56, doublet due to J_{56}; S, singlet (§, p =0.05).

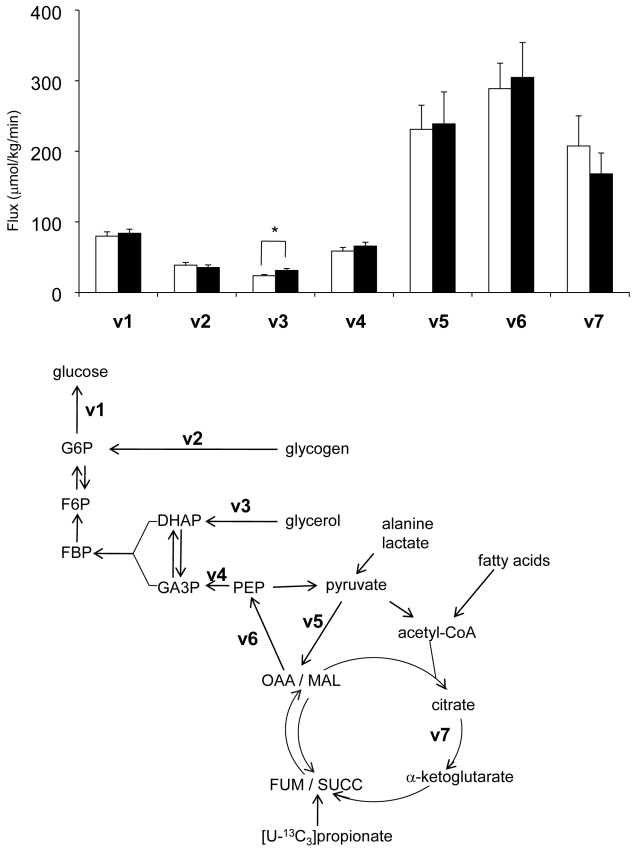

Figure 4.

Fluxes in the metabolic network supporting glucose production in controls (open, n=7-9) and high-fat-fed rats (black-filled, n=9). In the presence of ^2H_2O, glucose released from the liver may be enriched at positions H2 (G6P F6P), H5 (G3P DHAP), and $H6_s$ (OAA MAL), depending on the sources of gluconeogenic substrates. A three-day high-fat diet induced increased glycerol-gluconeogenesis without increasing basal glucose production and other supporting fluxes. (*, $p < 0.05$).

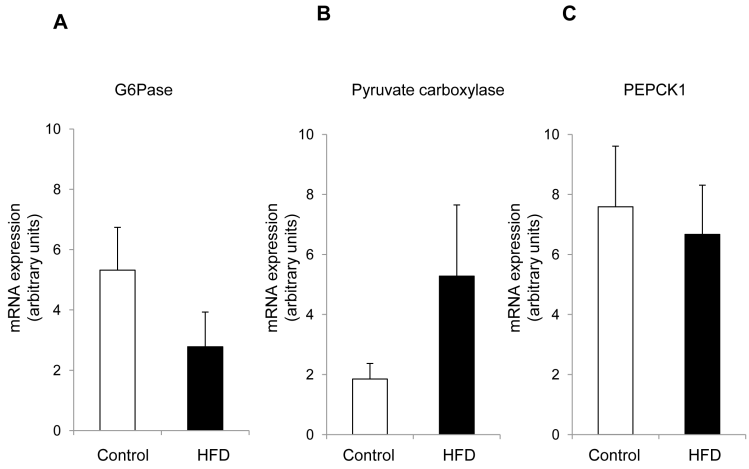

Figure 5.

Glucose 6-phosphatase (G6Pase), pyruvate carboxylase and PEPCK1 (cytosolic) expression from the liver of controls (n=6) and high-fat-fed rats (n=5). The levels of mRNA expression of G6Pase (**A**), pyruvate carboxylase (**B**) and PEPCK1 (**C**) were not statistically different between two groups.

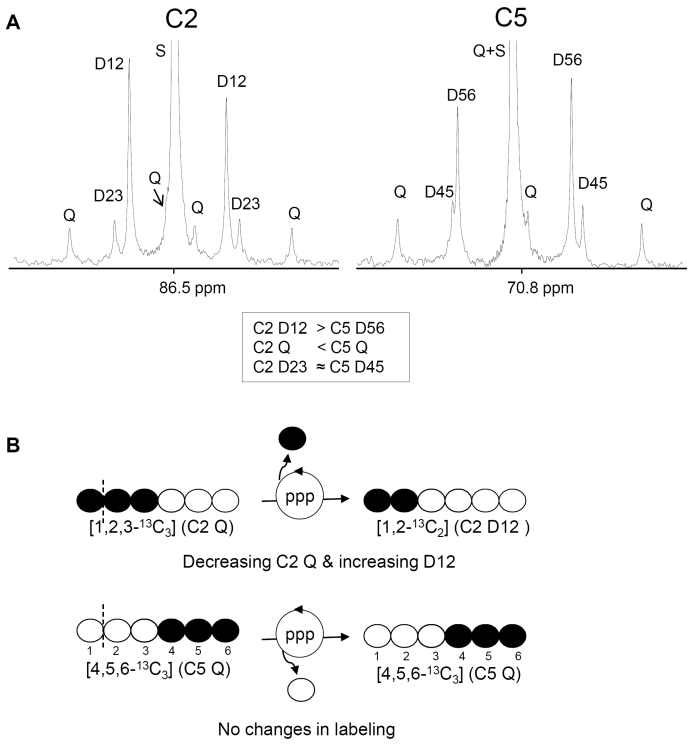

Figure 6.

C2 and C5 regions of ^{13}C NMR spectrum of MAG derived from plasma glucose of a high-fat-fed animal. Relative peak area of D12 is bigger than that of D56 while C2Q is smaller than C5Q (**A**). The ^{13}C asymmetry in glucose could be the activity of pentose phosphate pathway (PPP, **B**). MAG C5 resonance (rather than C2) was used in the analysis of fluxes associated with the citric acid cycle because the labeling at glucose C4-C6 remains the same even in the presence of PPP activity, reflecting the labeling of oxaloacetate C1-C3. See the text for the details. Abbreviations: D12, doublet due to J_{12}; D23, doublet due to J_{23}; Q, doublet of doublets, or quartet, arising from coupling of carbon 2 with both carbons 1 and 3 or from coupling of carbon 5 with both carbons 4 and 6; D45, doublet due to J 45; D56, doublet due to J_{56}; S, singlet resonance; open circle=^{12}C; filled circle=^{13}C.

Table 1

Characteristics of 4-5-hr fasted rats after a three-day high-fat diet (HFD). Blood and tissues were harvested at the end of [3,4-$^{13}C_2$]glucose infusion. Values represent mean ± SE for n=9 unless otherwise specified.

	Control	HFD
Body weight (g)	324 ± 4	338 ± 8
Plasma		
Glucose (mM)	11.3 ± 0.3	11.7 ± 0.3
Glycerol (mM)	1.3 ± 0.2	2.5 ± 0.2#
Triglycerides (μg/ml)	529 ± 81	445 ± 25
NEFAs (mM)	0.28 ± 0.04	0.35 ± 0.02
Insulin (ng/ml)	3.5 ± 0.4	6.4 ± 1.2*
Liver		
Triglycerides (mg/gww)	5 ± 2 (n=6)	34 ± 6# (n=5)
Glycogen(μmol glucosyl unit/gww)	164 ± 25 (n=8)	123 ± 11
Lactate (μmol/gww)	1.61 ± 0.10	1.69 ± 0.08
Pyruvate (μmol/gww)	0.61 ± 0.02	0.60 ± 0.03
[3,4-$^{13}C_2$]glucose enrichment		
Plasma glucose (%)	1.27 ± 0.08	1.22 ± 0.10
Liver glycogen (%)	NA (n=3)	NA (n=3)
Skeletal muscle glycogen (%)	0.05 ± 0.00 (n=3)	0.06 ± 0.01(n=3)
^{2}H enrichment in glucose H2 position		
Liver glycogen	NA (n=3)	NA (n=3)

*, #Significantly different from controls

*(, $p < 0.05$;

#, $p < 0.01$).

NA, natural abundance

Table 2

Relative and absolute values of EGP and supporting fluxes after a three-day high-fat diet (HFD). EGP was measured using the dilution of [3,4-13C2]glucose in plasma glucose by 13C NMR. Fractional sources of blood glucose were determined by the deuterium (2H) enrichments in glucose H2, H5 and H6s positions using 2H NMR analysis. Fluxes relative to citrate synthase flux (CS) were based on glucose C5 resonance analysis by 13C NMR. Notations for fluxes, v1 – v7, are illustrated in Figure 4. Values represent mean ± SE for n=9 unless otherwise specified.

	Control	HFD
EGP (v1,mmol/kg/min)	79.9 ± 6.0	83.8 ± 5.9
Fractional sources of blood glucose		
Glycogen	0.48 ± 0.02	0.41 ± 0.02
Glycerol	0.15 ± 0.01	0.19 ± 0.01§
PEP	0.37 ± 0.02	0.40 ± 0.02
Fluxes relative to citrate synthase		
gluconeogenesis/CS (v4/v7)	0.33 ± 0.06 (n=7)	0.46 ± 0.05
(PK+ME)/CS (v5/v7)	1.20 ± 0.13 (n=7)	1.42 ± 0.06
PEPCK/CS (v6/v7)	1.53 ± 0.15 (n=7)	1.88 ± 0.09§
Derived fluxes (mmol/kg/min)		
Glycogenolysis, v2	38.7 ± 3.9	35.3 ± 3.8
Glycerol→glucose,v3	23.7 ± 1.6	31.2 ± 2.7*
PEP → glucose, v4	58.7 ± 5.1	65.8 ± 5.4
PEP or malate→ pyruvate, v5	231.3 ± 34.1 (n=7)	239.0 ± 45.2
OAA → PEP, v6	288.9 ± 36.1(n=7)	304.8 ± 49.5
OAA → citrate, v7	207.5 ± 42.8 (n=7)	168.2 ± 29.4

§ $p = 0.05$

* significantly different from controls ($p < 0.05$).